

Combustion Regimes of Low-Lewis-number Counterflow Premixed Flames

Roman Fursenko^{1,2}, Sergey Minaev², Kaoru Maruta³, Hisashi Nakamura³

¹Khristianovich Institute of Theoretical and Applied Mechanics, SB RAS, Novosibirsk, Russia

²Far Eastern Federal University, Engineering School, Vladivostok, Russia

³Institute of Fluid Science, Tohoku University, 2-1-1 Katahira, Aoba, Sendai, 980-8577 Japan

1 Introduction

Although there is extensive literature on flammability limits of stretched premixed flames certain aspects of near-limit behavior of low-Lewis-number flames remain incompletely explored. Difficulties arising in the fundamental investigations of near-limit lean premixed flames are attributed not only to complex interaction of transport, chemical processes and radiative heat losses, but also to complex spatial structure of combustion wave is subjected to thermal-diffusive instability. The fuel-lean, near-limit laminar flames are sensitive to radiative heat losses which intensify thermo-diffusion instability resulting in the formation of non-planar cellular structures. Numerical simulations of the flame dynamics in straight [1] and divergent [2] channels showed that under the influence of radiative heat losses the low-Lewis-number flames break up to separate flame cells existing in a state of chaotic self-motion and splitting. In such systems, the combustion wave consists of separate cap-like fragments which sometimes close upon themselves to form seemingly spherical structures, that are allied to “flame balls” found in microgravity experiments [3]. Such combustion wave may be termed a “sporadic combustion wave” to distinguish its special properties that are different from properties of conventional continuous flame. One of the unusual features of sporadic combustion wave is incomplete burning of fuel that remains in the combustion products [2].

Radiative counterflow premixed flame is one of the basic objects for investigations of laminar flames structure. The results of microgravity experiments and theoretical investigations of stretched premixed flames with general Lewis numbers are widely presented in literature [4-7]. At the same time there is a lack of fundamental knowledge on dynamical behavior of low-Lewis-number stretched premixed flames. In the recent work of the authors [8] the characteristic combustion regimes of lean counterflow flames were investigated experimentally and numerically. It was found that 3D single-step Arrhenius kinetic thermal-diffusion model is capable to describe the main features of near-limit low-Lewis-number stretched flames observed in microgravity experiments. Since the 3D numerical simulations of the reactive flows with detailed chemistry are extremely time consuming procedure the use of reduced model seems to be reasonable for qualitative investigation of the complex flame behavior in the wide range of parameters.

In the present study the characteristics of lean counterflow premixed flames with radiative heat losses are studied numerically. The distinctive features of different combustion regimes are described and the regime diagram in the equivalence ratio / stretch rate plane is plotted.

2 Mathematical model

The 3D configuration considered in the present study is back-to-back counterflow premixed flames. In this configuration the air–fuel mixtures are issued from two opposed burners placed in positions $y=\pm L_y$ forming two flames near the stagnation plane $y=0$. It is assumed that the stagnation plane $y=0$ is a plane of symmetry. The following conventional framework of the model is employed: one-step exothermic reaction with Arrhenius kinetics, reactant composition far from stoichiometric, and radiative heat loss. With these assumptions, the appropriately nondimensionalized set of equations for temperature and deficient reactant concentration reads

$$T_t + \vec{\nabla} T = \nabla^2 T - h(T^4 - \sigma^4) + (1 - \sigma)W(T, C) \quad (1)$$

$$C_t + \vec{\nabla} C = Le^{-1} \nabla^2 C - W(T, C) \quad (2)$$

Here T is the scaled temperature in units of T_b , the adiabatic temperature of combustion products; C is the scaled concentration of the deficient reactant in units of C_0 - the value in the fresh mixture; x, y, z is non-dimensional spatial coordinates in units $l_{th}=D_{th}/U_b$, the thermal width of flame, where D_{th} is the thermal diffusivity of the mixture and U_b is the velocity of a planar adiabatic flame; t is the scaled time in units D_{th}/U_b^2 ; $\sigma = T_0/T_b$ where T_0 is the fresh mixture temperature; $Le=D_{th}/D_{mol}$ is the Lewis number, where D_{mol} is the deficient reactant molecular diffusivity. Dimensionless flow velocity vector in units U_b is given by formula $\vec{v}=(ax/2, -ay, az/2)$ where a is the non-dimensional stretch rate. Normalized chemical reaction rate has the following form $W(T, C)=(1-\sigma)^2 N^2 C \exp(N(1-1/T))/2Le$ where $N=T_a/T_b$ is the scaled activation energy and T_a is the activation temperature. At large N , the non dimensional velocity of planar adiabatic flame is close to unity in these variables. Unit value of non-dimensional flame speed corresponds to the dimensional velocity $U_b=B \exp(-T_a/2T_b)$ of a planar adiabatic flame in the high activation energy limit. The activation temperature T_a and pre-exponential factor B in the above formula were chosen to fit the dependence of U_b on equivalence ratio calculated by detailed reaction mechanism GRI-Mech 3.0. The term $h(T^4 - \sigma^4)$ in Eq. (1) represents radiative heat losses where h is scaled Stefan–Boltzmann constant in units of $\rho_b c_p l_p U_b / 4T_b^3 l_{th}$; l_p is the Planck mean absorption length; c_p , specific heat; ρ_b , burned gas density.

Equations (1) and (2) are considered in the rectangular domain $-L_x \leq x \leq L_x$, $0 \leq y \leq L_y$, $-L_z \leq z \leq L_z$ and subject to the following boundary conditions

$$\text{Inlet } (y=L_y): T=\sigma; C=1 \quad (3)$$

$$\text{Symmetry plane } (y=0): \partial T/\partial y=0; \partial C/\partial y=0 \quad (4)$$

$$x=\pm L_x, z=\pm L_z: T=\sigma; C=0. \quad (5)$$

Notice that asymmetrical flame configurations which may appear in experiments with two counterflow burners can not be reproduced due to restrictions imposed by symmetric boundary conditions (4).

The set of governing equations (1)-(2) was solved numerically by explicit finite-difference scheme. At initial moment, the computational domain is filled by fresh mixture with temperature σ . In the numerical simulations, the flame was ignited by specifying the high temperature zone near the stagnation plane. Five sets of the orthogonal grids of 256x192x256, 320x240x320, 384x288x384, 400x304x400 and 416x320x416 were employed. Convergence tests showed that the results of calculations for the three last-named finer grids are qualitatively the same and quantitative difference in flame speed $V_f=ay_f$ of adiabatic flame ($h=0$) was less than 0.2%. The solutions presented below correspond to the 384x288x384 grid and they were evaluated for $L_y=60$, $L_x=L_z=40$, $\sigma=0.2$, $N=10.5$.

The parallel computations of 3D problem on the base of GPU were realized. This technique allows significantly decrease computation time (about 50 times speedup) in comparison with

computations on conventional CPU. It makes possible effective 3D simulations on ordinary PC with graphic card without recourse to supercomputer.

3 Results and discussion

The big variety of flame patterns was revealed in simulations of lean stretched premixed flames with radiative heat losses. It is necessary to notice that 2D simulations does not allow to describe all variety of combustion regimes. In 3D simulations the planar counterflow flames (see Fig. 1a) was observed for the respectively high stretch rates and equivalence ratios. Decreasing of the stretch rate leads to the flame front cellularization (see Fig. 1b) due to the increasing influence of thermal-diffusive instability. In these cases, the flame represents by continuous surface separating unburned gas and combustion products and it is possible to determine the mean flame front position by time averaging y coordinate of the flame surface. As one would expect, continuous flame consumes the deficient reactant completely.

In the range of respectively small equivalence ratios and stretch rates, the flame front structure gradually changed in the same manner as it was described in [9] for the lean low-Lewis-number flame

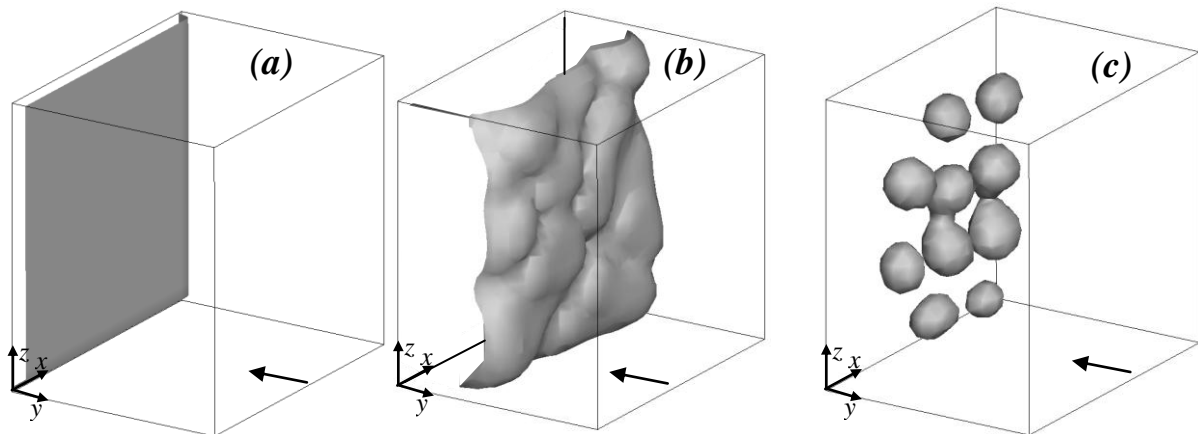


Figure 1. Typical flame structures (equiscalar surfaces $T=0.6$ are depicted) of planar (a), cellular (b) and sporadic (c) counterflow flames.

propagating in the straight channel. With decreasing of equivalence ratio, the cell size increases at first, after that the cellular flame suffers local extinction at some of its cusps accompanied by a noticeable escape of the unconsumed reactant through the emerging gaps. For sufficiently lean mixtures, the cellular flame disintegrates into a group of nearly identical cells resembling flame balls (see Figs.1c). Their mutual arrangement however is not frozen but involves fluctuations, sporadic detachments of the leading cell from the others, followed by its disintegration and formation of the secondary cells that are nearly identical to the primary one. As a rule after the splitting, one of the ball-like flames is moved downstream with the flow and eventually disappears due to gradual depletion of the mixture.

In spite of this moving, splitting and extinguishing of ball-like flames, the equiscalar fuel concentration surfaces before combustion zone remain smooth surfaces. These surfaces being time averaged over characteristics intervals of several ball-like flame disintegrations are almost flat. Thus, it makes possible to attribute averaged flame front position and velocity to an array of ball-like flames observed in experiments and numerical simulations.

The dependence of the flame front speed on dimensionless fuel concentration $1/\sigma-1=T_b/T_0-1=(T_0+Q/c_p \cdot Y_\infty)/T_0-1= Y_\infty Q/(T_0 c_p)$ where Y_∞ is the initial fuel mass fraction is shown in (Fig.2a). Notice that flame velocity in Fig.2a was calculated for distant flames located far from stagnation plane. The flame speed of distant flames remains almost constant with variation of stretch rate. As it may be concluded from Fig. 2b the flame front velocity is increasing function of nondimensional parameter $1/\sigma-1$. Since the distance between the counterflow flames is proportional to V_f at fixed stretch rate, it increases with increase of $1/\sigma-1$. This result coincides with experimental observations presented in [8].

Figure 2b shows dependency of unconsumed reactant concentration on non-dimensional fuel concentration in fresh mixture. At respectively low equivalence ratios the incomplete fuel consumption is observed and the fuel leakage increases with decrease of equivalence ratio at fixed stretch rate. This effect induces by increasing of the gap between the flame cells with premixture

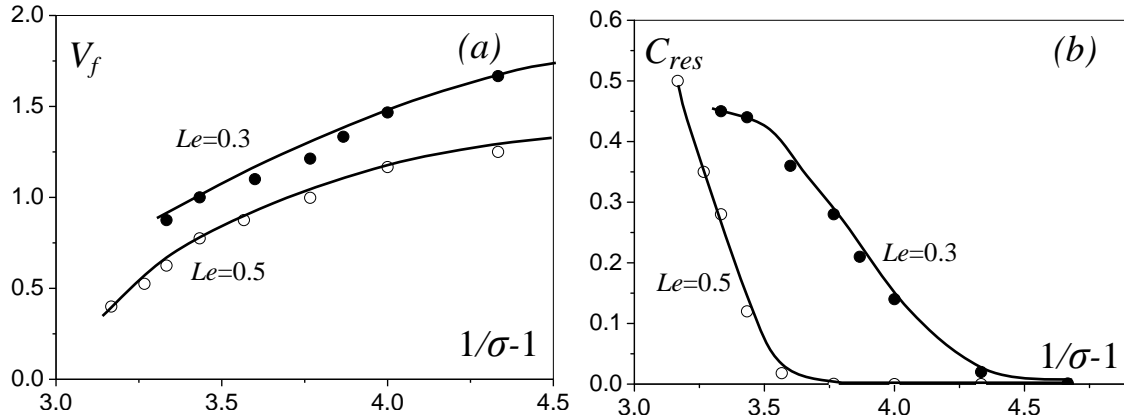


Figure 2. Dependences of the flame propagation velocity V_f (Fig.2a) and concentration of unconsumed reactants C_{res} (Fig.2b) on dimensionless fuel concentration $1/\sigma-1$.

thinning. (see Fig. 1b,c). The average flame balls radius decreases with increasing of the heat-loss rate that coincides with theoretical predictions obtained for the isolated flame ball in free space [10] and with numerical results obtained for the flame balls in a divergent channel [2].

Numerical simulations showed that the flame can be established in stagnation flow field in the wide range of problem parameters such as stretch rate, mixture contents and heat-loss intensity. The flame speed and regions of flame existence strongly depend on Lewis number as seen in Fig. 2a. Decreasing of the Lewis number leads to the widening of the flammability limits (see Fig. 2a) due to effect of thermal-diffusion instability which becomes stronger with decreasing of Lewis number. Such flame behavior was predicted theoretically for non-adiabatic cellular flame [11].

Regime diagram in the equivalence ratio/stretch rate plane calculated for $Le=0.5$ is presented in Fig. 3. The non-dimensional regime diagram is presented in incut in Fig. 3. Solid line corresponds to

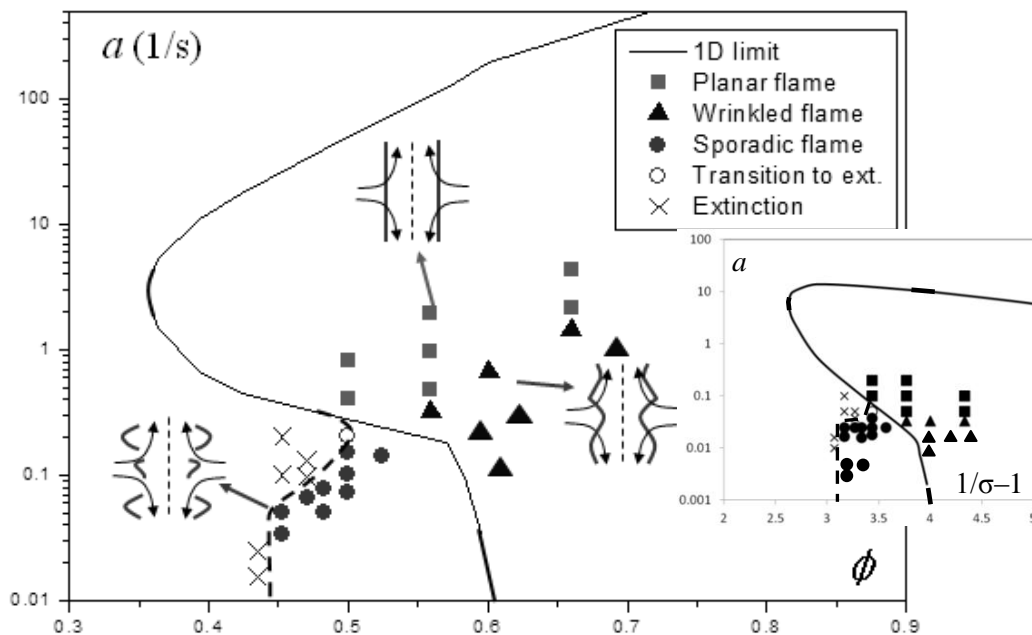


Figure 3. Regime diagram in equivalence ratio - stretch rate plane and regime diagram in non-dimensional form (incut)

the flammability limits of 1D stretched flame calculated in the frame of thermal-diffusion model with one-step reaction. The flammability limits are in a good agreement with the results of 1D simulations with detailed chemistry described by GRI 3.0 mechanism. Inside the C-shape curve bounded the region of 1D flame existence the continuous flame front is observed. In this region the fuel is completely consumed. At low stretch rates the flame front has a cellular structure (triangles in Fig.3) due to thermal-diffusion instability. At respectively high stretch rates the planar flame exists (bars in Fig.3) because of suppression of thermal-diffusion instability by flow. The planar flame may be well described in the frame of 1D model. At low stretch rates the sporadic combustion wave is represented by the set of moving ball-like flames which may exist beyond the flammability limits of 1D counterflow flame (circles at Fig.3.). This fact may be explained by reduction of the total radiative heat losses from the combustion products region and the flame curvature effects being peculiar to the flame ball-like structures. The significant fuel leakage is observed in the region of parameters corresponding to the sporadic regime of combustion. Regime diagram for $Le=0.3$ is qualitatively the same as that one for $Le=0.5$. It may be concluded that thermal-diffusion instability at low-Lewis-numbers leads to the extension of the flammability limits of premixed flames through the sporadic combustion regime. It may be supposed that accounting for detailed mechanism of reactions may results in quantitative change of regime diagram but qualitative behavior of the flame remains the same because the main mechanisms governing flame behavior is thermal-diffusive instability in presence of radiative heat losses.

4 Conclusions

Dynamical behavior of the low-Lewis-number lean premixed flames with radiative heat losses propagating in stagnation-plane flow has been investigated numerically. Dependencies of the flame structure, flame position, flame speed and unconsumed reactant concentration on the heat losses intensity and stretch rate were obtained. Numerical simulations of lean low-Lewis-number stretched premixed flames detected that combustion wave can consist of separate combustion zones resembling flame balls. In this regime essential incompleteness of combustion was observed. This incompleteness occurs in the process of lean mixtures' combustion and is caused by fuel leakage through the gaps among ball-like flames. It was found that the concept of flame front may be extended to the case of separate flame balls that makes possible to characterize complex behavior of interacting flame balls by one general parameter. Averaged flame position may be considered as a convenient characteristic of lean gas combustion for models verification.

The regions of existence of different combustion regimes in equivalence ratio/stretch rate plane were determined. The extension of flammability limits associated with existence of sporadic combustion regimes has been detected. The numerical results qualitatively coincide with experimental observations that justify the use of reduced model and allow us to distinguish the main physical processes governing flame behavior.

5 Acknowledgments

The work was partially supported by Integration project SB RAS - FEB RAS No.38.

References

- [1] Kagan L, Sivashinsky G. (1997). Self-fragmentation of nonadiabatic cellular flames. *Combust. Flame.* 108: 220.
- [2] Fursenko R, Minaev S. (2011). Flame balls dynamics in divergent channel. *Combust. Theory and Model.* 15: 817.
- [3] Ronney PD. (1990). Near-limit flame structures at low Lewis number. *Combust. Flame.* 82: 1.

-
- [4] Maruta K, et al. (1996). Experimental study on methane-air premixed flame extinction at small stretch rates in microgravity. 26th Symp. (Int.) Combust.: 1283.
 - [5] Ju Y, et al. (1997). On the extinction limit and flammability limit of non-adiabatic stretched methane-air premixed flames. *J. Fluid. Mech.* 342: 315.
 - [6] Ju Y, et al. (1998). Flame bifurcations and flammable regions of radiative counterflow premixed flames with general Lewis numbers. *Combust. Flame* 113: 603.
 - [7] Buckmaster JD. (1997). The effects of radiation on stretched flames. *Combust. Theory Modell.* 1: 1.
 - [8] Fursenko R, et al. (2013). Cellular and sporadic flame regimes of low-Lewis-number stretched premixed flames. *Proc. Combust. Inst.* 34: 981.
 - [9] Kagan L, Minaev S, Sivashinsky G. (2004). On self-drifting flame balls. *Math. and Comp. in Sim.* 65: 511.
 - [10] Buckmaster J, Joulin G, Ronney P. (1990). The structure and stability of nonadiabatic flame balls. *Combust. Flame.* 79: 381.
 - [11] Joulin G, Sivashinsky GI. (1983). On the dynamics of near-extinguished non-adiabatic cellular flames. *Combust. Sci. Technol.* 31: 75.